

Noise Isolation in LTCC-based X/Ku-band Transceiver SiP using Double-Stacked Electromagnetic Bandgap Structure

Jongbae Park, *Junchul Kim, **Albert Chee W. Lu, Yujeong Shim, and Joungho Kim

Terahertz Interconnection and Package Lab., Dept. of EECS, Korea Advanced Institute of Science and Technology, 373-1 Guseong, Yuseong, Daejeon 305-701, South Korea, E-mail: pjb77@eeinfo.kaist.ac.kr

*Korea Electronics Technology Institute, Seongnam, 463-816, South Korea

**Singapore Institute of Manufacturing Technology, 71 Nanyang Drive, Singapore 638075

Abstract—We experimentally investigate the isolation effect of the noise coupling in X/Ku-band transceiver SiP fabricated on low-temperature co-fired-ceramic (LTCC) multilayer substrate, using a double-stacked electromagnetic bandgap (DS-EBG) structure. The fabricated transceiver SiP is composed of Ku-band transmitter and X/Ku-band receiver. To prevent the simultaneous switching noise coupling from digital circuits, a DS-EBG structure was designed and implemented to the transceiver SiP. The effect of DS-EBG, which gives 30 dB stopband over X/Ku-band ranges, was demonstrated through frequency and time domain measurement.

Keywords – *Electromagnetic Bandgap Structure, EBG, DS-EBG; Power/Ground SSN; X/Ku-band; Transceiver; System-in-Package; SiP*

I. INTRODUCTION

As the significant worldwide demand for higher data rates and broadband transmission increases, applications of satellite communication systems over GHz range are expanding. However, the current drawbacks of most commercially available millimeter wave front-ends are their relatively large size and heavy weight which are caused by discrete components such as filters, and separately located module. Thus the implementation of a compact transceiver system-in-package (SiP) is the key issue for reduction in cost, size, and system complexity. The SiP has countless closely spaced metallic interconnection structures such as traces, vias, pads, leads, partial planes, and plane cavities in a small package. These densely spaced interconnection structures become sources of high frequency noise generation and noise coupling, imposing serious signal and power integrity issues as well as EMI/EMC problems [1-2]. Problems arise with high-speed and high-density multilayer PCBs, where many RF, analog and digital devices are integrated into a densely populated package. The noise at the SiP or the PCB worsens noise and timing margin of digital and analog circuits, resulting in reduction of achievable jitter performance, Bit Error Rate (BER) and system reliability. The coupled noise from fast switching digital devices can also affect phase noise and Signal to Noise Ratio (SNR) performance in RF and wireless communication circuits. In high-speed and high-density SiPs and PCBs, a major element of the high frequency noise is simultaneous switching noise (SSN) from fast-switching digital circuits, as

clock frequencies and the amount of switching current are significantly increased [3]. Therefore, there have been various efforts to isolate the SSN coupling between digital and analog circuits [4-6]. First of all, conducting neck structure has been used to isolate the SSN coupling, guaranteeing the DC connection between digital and analog power. Analogous to the conducting neck structure, ferrite beads can be also used because it blocks high frequency signal or noise and connects DC signal. However, these methods to isolate SSN coupling have limitations that those guarantees the isolation in a narrow band of low frequency range. As such limitations, electromagnetic bandgap (EBG) structure has been emerged as an alternative solution to highly isolate the SSN coupling between digital and analog circuits. The EBG structures are periodic structures in which the propagation of electromagnetic waves is forbidden in certain frequency bands. A common feature of periodic structures is the existence of frequency bands where electromagnetic waves are highly attenuated and do not propagate [7]. Several papers have discussed the use of high-impedance surfaces (HISs) and high-dielectric thin films in EBG structures [7-15]. These EBG structures have been implemented on an inner metal layer embedded between the power and ground planes. In addition, cascaded EBG structures with different cell sizes have been used to increase the bandwidth of the EBG bandgap [7, 11-12]. Furthermore, in our previous paper [16], a new EBG structure with a significantly extended noise isolation bandwidth for mixed-signal SiP applications, called a double-stacked EBG (DS-EBG) structure, fabricated on an LTCC multilayer substrate was introduced. In this paper, we experimentally investigate the isolation effect of the DS-EBG structure in X/Ku-band transceiver SiP fabricated on low-temperature co-fired-ceramic (LTCC) multilayer substrate. The fabricated transceiver SiP is composed of Ku-band transmitter and X/Ku-band receiver. To prevent the simultaneous switching noise coupling from digital circuits, a DS-EBG structure was designed and implemented to the transceiver SiP. The effect of DS-EBG, which gives 30 dB stopband over X/Ku-band ranges, was demonstrated through frequency and time domain measurement.

II. DESIGN OF LTCC-BASED X/KU-BAND TRANSCEIVER

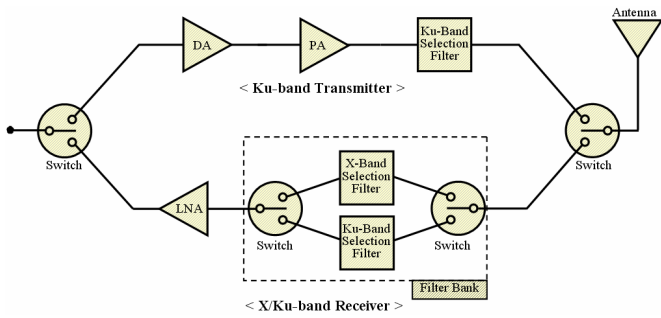


Figure 1 Block diagram of RF front-end X/Ku-band Transceiver

Operations	Center Frequency	Bandwidth
Transmitter (Ku-band Operation)	14.25 GHz	500 MHz
Receiver	X-band Operation	9.25 GHz
	Ku-band Operation	14.25 GHz

Figure 2 Center frequency and bandwidth of X/Ku-band transceiver SiP

We have designed a low cost, compact, and small size X/Ku-band transceiver SiP using low temperature co-fired ceramic (LTCC) process. LTCC technology is the preferred platform for high-performance SiP because of its superior high frequency characteristics and its high integration capability. That's why we used the LTCC technology to design X/Ku-band transceiver SiP. The block diagram of the designed LTCC-based X/Ku-band transceiver is shown in Figure 1. As shown in the figure, the transceiver is composed of Ku-band transmitter and X/Ku-band receiver. We have integrated all components of the block diagram except antenna in a single package using LTCC process. To isolate Ku-band transmitter and X/Ku-band receiver, four switches with over 30 dB isolation level were used. Ku-band transmitter of the designed transceiver has a center frequency of 14.25 GHz and a bandwidth of 500 MHz, and X/Ku-band receiver of the designed transceiver has a center frequency of 9.25 GHz and 14.25 GHz, respectively, and a bandwidth of 500 MHz, as shown in Figure 2.

The transmitter's power budget along the signal path is shown in Figure 3. As shown in the figure, the transmitter has an output power of 28.5 dBm, i.e. 700 mW. The information of the components including the switch, drive amplifier, power amplifier, and filter is shown, as well. We have selected the proper components to satisfy with the power budget of the transmitter, and the overall transmitter gain is 41.5 dB. The receiver's power budget along the signal path is shown in Figure 4. The power budget for receiver was given by calculating the minimum detectable signal power of the receiver. As shown in Figure 4, the calculated minimum detectable signal power of the receiver was -73 dBm. With reference to the signal power, we selected the proper components including switch, low noise amplifier, filter. The overall gain and noise figure of the receiver is -5 dBm and 14 dB, respectively. The noise figure is very high because of the use of filter bank. Especially, the receiver has to operate over

X-band as well as Ku-band so that the LNA should operate in a wide frequency range resulting in the increase of its noise figure.

	Switch	Drive Amp.	Power Amp.	Filter	Switch
Gain (dB)	-2.5	16.5	33	-3	-2.5
Input RL (dB)	9	15	11	11	9
Output RL (dB)	11	13	15	11	11
Total Gain (dB)	-2.5	14	47	44	41.5
P [out] (dBm)	-15.5	1	34	31	28.5
Selected Die	TGS2306	TGA2506	TGA2503	Buried Type	TGS2306

* 0.7 Watt Output Power

Figure 3 Power budget of transmitter.

	Switch	Switch	Filter	Switch	LNA	Switch
Gain (dB)	-2.5	-2.5	-3	-2.5	8	-2.5
NF (dB)	2.5	2.5	3	2.5	3.5	2.5
Input RL (dB)	9	9	11	9	16	9
Output RL (dB)	11	11	11	11	17	11
Total Gain (dB)	-2.5	-5	-8	-10.5	-2.5	-5
NF [out] (dB)	2.5	5	8	10.5	14	14
P [out] (dBm)	-75.5	-78	-81	-83.5	-75.5	-78
Selected Die	TGS2306	TGS2306	Buried Type	TGS2306	TGA1342	TGS2306

* Minimum Detectable Signal Power =kTB·F=-73 dBm

Figure 4 Power budget of receiver.

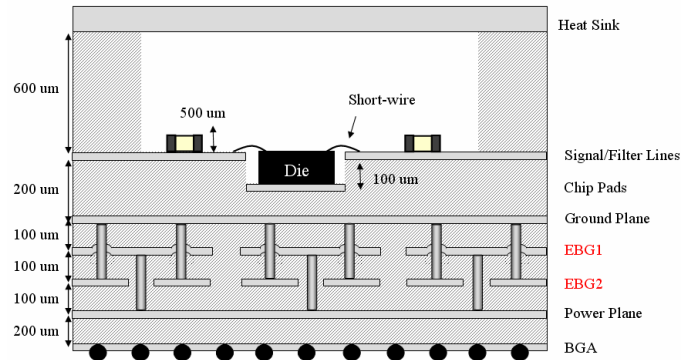


Figure 5 Stack-up of the designed X/Ku-band transceiver SiP.

All components for X/Ku-band transceiver design are integrated in a single package which stack-up is shown in Figure 5. Since the transceiver SiP uses LTCC process, it is possible to increase, cost-effectively, the number of transceiver layers as much as we desire. The stack-up for the transceiver SiP has 8 layers, which is consisted of BGA layer, power plane layer, EBG1 layer, EBG2 layer for the integration of the double-stacked electromagnetic bandgap (DS-EBG) structure, ground plane layer, Chip pad layer, signal/filter line layer, and heat sink layer. In particular, by using cavity process of the LTCC technology, it made it possible to embed all chips inside of the designed package, resulting in the reduction of wire-

bonding length. Figure 6 shows the top view of the designed X/Ku-band transceiver SiP. The thickness and size of the transceiver SiP are 1.3 mm and 20 mm x 20 mm, respectively. The dielectric constant and loss tangent of the SiP are 7.4 and 0.001, respectively. There are 7 chip-dies and 5 decoupling capacitors in the transceiver SiP.

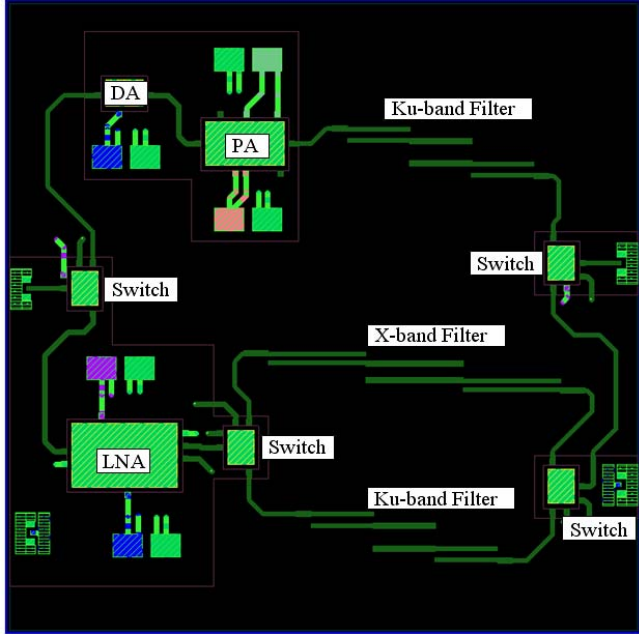


Figure 6 Top view of the designed X/Ku-band transceiver SiP

III. DESIGN OF DOUBLE-STACKED EBG STRUCTURE

In our previous paper [16], we proposed a novel EBG structure with a significantly extended noise isolation bandwidth for mixed-signal SiP applications, called a double-stacked EBG (DS-EBG) structure, fabricated on an LTCC multilayer substrate. Our design approach was enabled by combining two EBG layers embedded between the power and ground planes, as shown in Figure 7, while the two EBG layers had different bandgaps from using different cell sizes. The adoption of different EBG cell sizes in the upper EBG layer (EBG1) and the bottom EBG layer (EBG2) made it possible to extend the bandwidth of the DS-EBG bandgap, while still maintaining the same EBG surface area. Furthermore, the buried vias connecting EBG1 and EBG2 were laterally orientated with a staggered arrangement, as shown in Figure 7 (b), to increase the capacitance between the EBG cell plate and the opposite power or ground plane, resulting in an increased bandwidth of each EBG structure [12].

The DS-EBG structure was designed and implemented to the X/Ku-band transceiver SiP using a 100 μm thick low-loss LTCC dielectric and 10 μm thick silver conductors. The relative permittivity and loss tangent of the dielectric were 7.4 and 0.001, respectively. The EBG cells had dimensions of $1.4 \times 1.4 \text{ mm}^2$ for EBG1 layer and $2 \times 2 \text{ mm}^2$ for EBG2 layer, and

were arrayed in the TVs on an overall LTCC substrate size of $20 \times 20 \text{ mm}^2$.

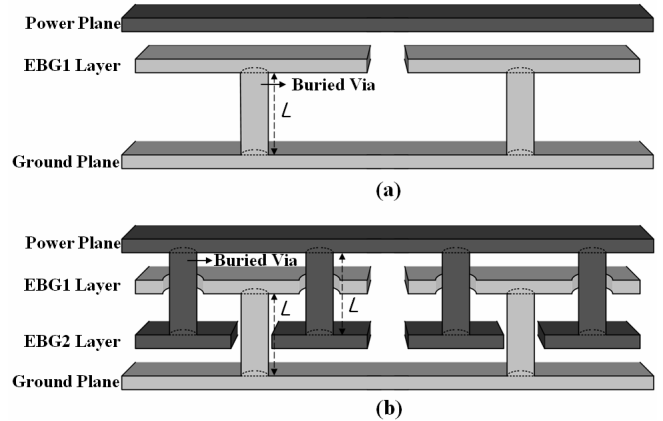


Figure 7 The side view of: (a) a previous EBG structure, and (b) our proposed DS-EBG structure to provide wide suppression of SSN coupling for LTCC-based SiP applications.

IV. MEASUREMENT RESULTS

We fabricated the designed X/Ku-band transceiver SiP using LTCC process, as shown in Figure 8. The figure shows the fabricated transceiver package, FR4-based test board, heat pipe, assembled module, and the assembled module with heat pipe. For the stable operation of the fabricated transceiver SiP, we have designed and fabricated the heat sink which has an excellent performance for the system with small size and high power consumption. The thermal resistance of the designed heat pipe is about $1.3 \text{ }^\circ\text{C/Watt}$. It means that, by using the heat pipe, the increase of heat is only $1.3 \text{ }^\circ\text{C}$ as the transceiver consumes 1 Watt power.

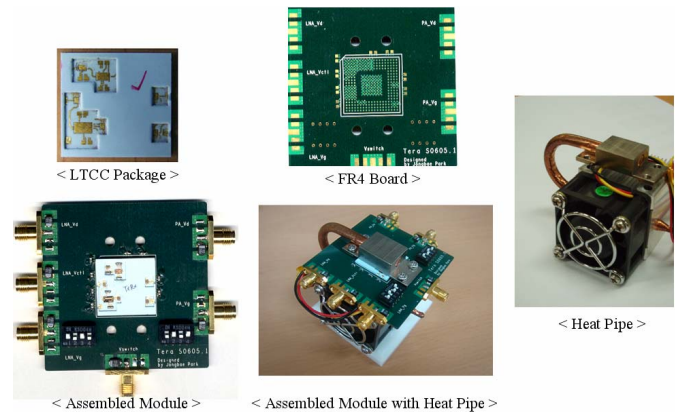


Figure 8 The fabricated LTCC package, FR4 board, assembled model, heat pipe, and assembled module with heat pipe.

We have used on-packaging probing to verify the transceiver performance. Six power supplies were needed to

operate 7 dies in the X/Ku-band transceiver. Vector network analyzer, spectrum analyzer, and noise figure analyzer were used with probe station using 400 um pitch probe. The comparisons of transceiver specification with the measurement results are shown in Figure 9. When the receiver is selecting X-band filter, the measured overall receiver gain is -5.4 dB, and the center frequency is 9.26 GHz, and the bandwidth is 500 MHz. When the receiver is selecting Ku-band filter, the measured overall receiver gain is -8.1 dB, the center frequency is 14.25 GHz, and the bandwidth is 500 MHz. Finally, the measured overall transmitter gain is 41.73 dB, the center frequency is 14.25 GHz, and the bandwidth is 800 MHz. We can see that the measurement results are satisfied with the transmitter's specification well.

		Specification	Measurement
Receiver (X-band)	Center Frequency	9.25 GHz	9.26 GHz
	Bandwidth	500 MHz	500 MHz
	Overall Gain	-5 dB	-5.4 dB
Receiver (Ku-band)	Center Frequency	14.25 GHz	14.25 GHz
	Bandwidth	500 MHz	500 MHz
	Overall Gain	-8 dB	-8.1 dB
Transmitter (Ku-band)	Center Frequency	14.25 GHz	14.25 GHz
	Bandwidth	500 MHz	800 MHz
	Overall Gain	41.5 dB	41.73 dB

Figure 9 The comparison of transceiver specification with the measurement.

To investigate the effect of the DS-EBG on the LTCC-based X/Ku-band transceiver's performance, we have integrated the DS-EBG structure in the transceiver. The DS-EBG structure was designed to have a stopband in X/Ku-band frequency range because the transceiver operates in X/Ku-band frequency range. Figure 10 shows the measured power/ground noise coupling coefficient, S21, in the fabricated transceiver SiP. From the results shown in figure, it was observed that the DS-EBG structure of the transceiver SiP had a stop bandwidth of about 9 GHz (below -30 dB) covering X/Ku-band frequency range.

To demonstrate the noise isolation effect of the DS-EBG structure against broadband SSN in X/Ku-band transceiver SiP, a 250 mV, 3 GHz clock signal was fed into the power/ground port. The coupled power/ground noise was measured at the output of the transceiver. First, X/Ku-band transceiver not integrating DS-EBG structure was measured to observe the effect of power/ground noise coupling. The observed output signals are shown in Figure 11. When there is no power/ground noise, the output signal has the expected value, -12.17 dBm. However, when a power/ground noise is excited, the output signal has a noise signal of -43 dBm at 8.999997 GHz, which is the third harmonic of the excited 3

GHz power/ground noise. Because the signal is quite close to the wanted signal, the noise will affect the system failure.

In the case of the X/Ku-band transceiver with DS-EBG structure, the unwanted signal was disappeared as shown in Figure 12. It is understood that the integrated DS-EBG structure successfully suppressed the unwanted signal power by 21 dB.

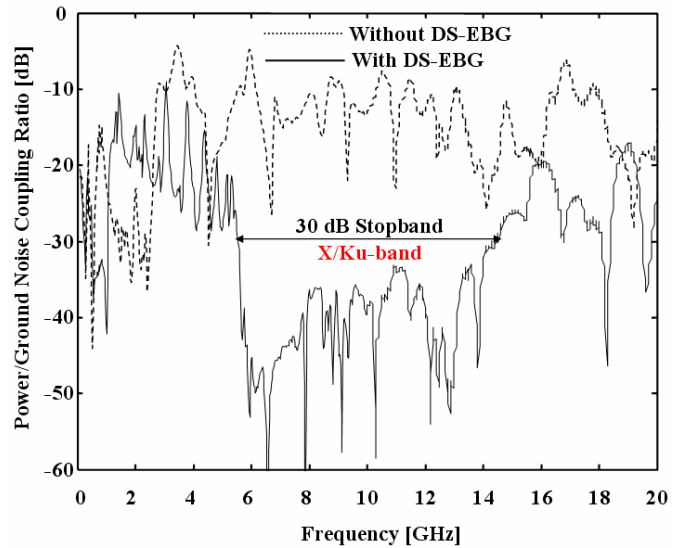


Figure 10 The measured power/ground noise coupling ratio, S21 up to 20 GHz; dotted line represents a X/Ku-band transceiver SiP without EBG structure, solid line represents a X/Ku-band transceiver SiP integrating double-stacked EBG structure.

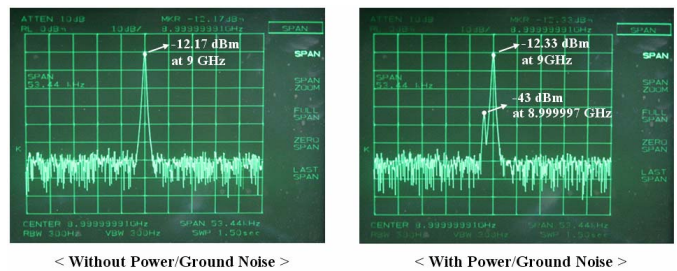


Figure 11 Measured output power with and without power/ground noise in the X/Ku-band transceiver not integrating DS-EBG.

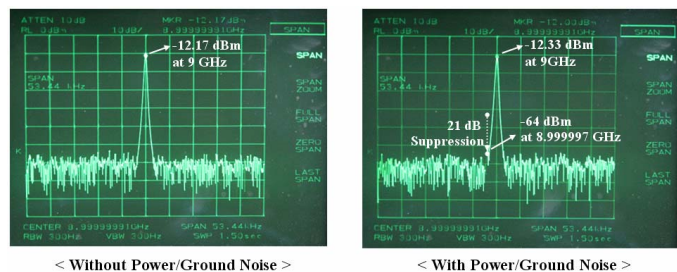


Figure 12 Measured output power with and without power/ground noise in the X/Ku-band transceiver integrating DS-EBG.

The noise figure was also observed because all of noisy RF and microwave components can be characterized by noise figure. Noise figure (F) is a measure of the degradation in the signal-to-noise ratio between the input and output of the component. Thus, the noise figure can be calculated by this equation.

$$F \text{ (dB)} = 10 \cdot \log\left(\frac{S_i / N_i}{S_o / N_o}\right) \geq 1 \quad (1)$$

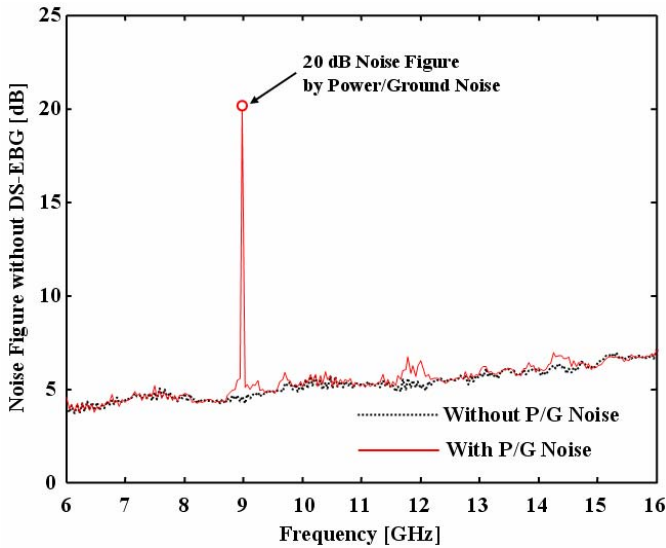


Figure 13 Measured noise figure in the X/Ku-band transceiver not integrating DS-EBG.

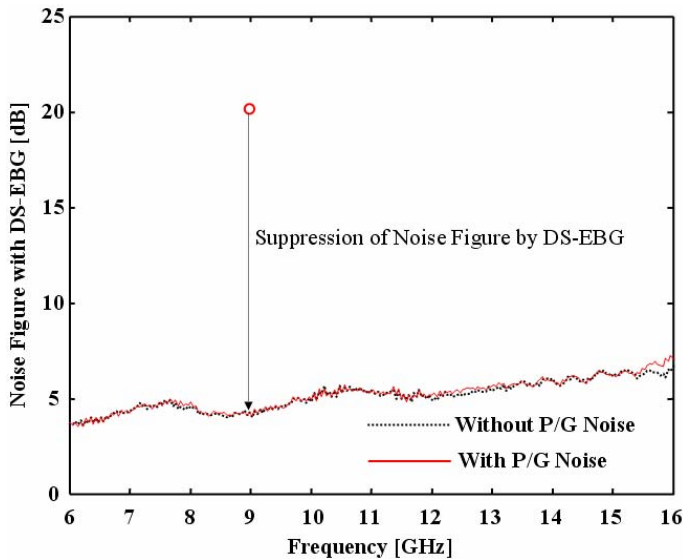


Figure 14 Measured noise figure in the X/Ku-band transceiver integrating DS-EBG.

First, X/Ku-band transceiver not integrating DS-EBG structure was measured to observe the effect of power/ground noise coupling on noise figure. The observed noise figures are shown in Figure 13. In the measured noise figure, when there is no power/ground noise, the noise figure is between 3 dB and 6 dB. However, once a power/ground noise is applied, the noise figure has very high value of 20 dB at 8.999997 GHz which is from the third harmonic of the excited 3 GHz power/ground noise. In the case of the X/Ku-band transceiver with DS-EBG structure, the high value of noise figure was disappeared as shown in Figure 14. It is understood that the integrated DS-EBG structure successfully suppressed the high value of noise figure caused by power/ground noise coupling.

V. CONCLUSION

In this paper, we have experimentally investigated the noise isolation effect of the DS-EBG structure in a X/Ku-band transceiver SiP fabricated on low-temperature co-fired-ceramic (LTCC) multilayer substrate. The fabricated transceiver SiP was consisted of Ku-band transmitter and X/Ku-band receiver. To prevent the simultaneous switching noise coupling from digital circuits, a DS-EBG structure was designed and implemented to the transceiver SiP. The effect of DS-EBG, which gives 30 dB stopband over X/Ku-band ranges, was demonstrated through frequency and time domain measurement. The integrated DS-EBG structure successfully suppressed the noise signal and the high value of noise figure caused by power/ground noise coupling.

REFERENCES

- [1] Sudo T, Sasaki H, Masuda N, and Drewniak J.L, "Electromagnetic Interference (EMI) of System-on-Package (SoP)", IEEE Transactions on Advanced Packaging, Vol. 27, Issue 2, pp. 304-314, May 2004.
- [2] Jongbae Park, Hyungsoo Kim, Youchul Jeong, Jinguok Kim, Jun So Pak, Dong Gun Kam, and Joungcho Kim "Modeling and Measurement of Simultaneous Switching Noise Coupling through Signal Via Transition", IEEE Transactions on Advanced Packaging, Vol.29, No.3, Aug. 2006, pp. 548-559
- [3] International Technology Roadmap for Semiconductors 2005.
- [4] H. Liaw and H. Merkelo, "Signal integrity issues at split ground and power planes", Proceedings of Electronic Components and Technology Conference, pp. 752-755, May 1996.
- [5] J. Choi, S. Min, J. Kim, M. Swaminathan, W. Beyene, and X. Yuan, "Modeling and analysis of power distribution networks for gigabit applications", IEEE Trans. Mobile Computing, vol. 2, no. 4, pp. 299-313, October-December 2003.
- [6] W. Cui, J. Fan, Y. Ren, Hao Shi, J. L.Drewniak, and R. E. DuBroff, "DC power-bus noise isolation with power plane segmentation", IEEE Trans. Electromagnetic Compatibility, vol 45, no. 2, pp.436-443, May 2003.
- [7] Jinwoo Choi, "Noise suppression and isolation in mixed-signal systems using alternating impedance electromagnetic bandgap (AI-EBG) structure", Ph. D Thesis, 2005.
- [8] R. Abhari, and G.V. Eleftheriades, "Metallo-dielectric electromagnetic bandgap structures for suppression and isolation of the parallel-plate noise in high-speed circuits," IEEE Transactions on Microwave Theory and Techniques, vol. 51, no. 6, pp. 1629-1639, Jun. 2003.
- [9] T. Kamgaing and O.M. Ramahi, "A novel power plane with integrated simultaneous switching noise mitigation capability using high

impedance surface,” *IEEE Microw. Wireless Compon. Lett.*, vol. 13, no. 1, pp. 21–23, Jan. 2003.

- [10] S. Shahparnia, and O.M. Ramahi, “Miniaturized electromagnetic bandgap structures for broadband switching noise suppression in PCBs,” *Electronics Letters*, vol. 41 no. 9, pp. 519–520, Apr. 2005.
- [11] S. Shahparnia and O.M. Ramahi, “Simultaneous switching noise mitigation in PCB using cascaded high-impedance surfaces,” *Electronics Letters*, vol. 40, no. 2, pp. 98–100, Jan. 2004.
- [12] S. D. Rogers, “Electromagnetic-Bandgap Layers for Broad-Band Suppression of TEM Modes in Power Planes,” *IEEE Transactions on Microwave Theory and Techniques*, vol. 53, pp. 2495–2505, Aug. 2005.
- [13] S. Shahparnia and O.M. Ramahi, “High-impedance surfaces embedded in printed circuit boards: design considerations and novel applications,” *IEEE Antennas and Propagation Society International Symposium*, vol. 4, pp. 3569–3572, June 2004.
- [14] S. Shahparnia, and O.M. Ramahi, “Miniaturized electromagnetic bandgap structures for ultra-wide band switching noise mitigation in high-speed printed circuit boards and packages,” in *Proc. IEEE 13th Topical Meeting on Electrical Performance of Electronic Packaging*, 2004, pp. 211–214.
- [15] J. Lee, H. Kim, and J. Kim, “High dielectric constant thin film EBG power/ground network for broadband suppression of SSN and radiated emissions,” *IEEE Microw. Wireless Compon. Lett.*, vol. 15, no. 8 pp. 505–507, Jan. 2003.
- [16] J. Park, A. C. W. Lu, K. M. Chua, L. L. Wai, J. Lee, and J. Kim, “Double-Stacked EBG Structure for Wideband Suppression of Simultaneous Switching Noise in LTCC-based SiP Applications,” *IEEE Microw. Wireless Compon. Lett.*, vol. 16, no. 9, pp. 481–483, Sep. 2006